

Open-pore MFI zeolite nanosheets modified separator with Li-ion flux regulation for lithium-metal batteries

Yunyun Zhai,^{a, b, #} Yunqin Wu,^{a, #} Junlu Sheng,^c Haiqing Liu,^{a, *} Zhenpeng Huang,^a
Qiang Xiao^{d,*} and Lei Li^{a,*}

^a Jiaying Key Laboratory of Molecular Recognition and Sensing, College of Biological, Chemical Sciences and Engineering, Jiaying University, Jiaying, 314001, China

^b Research Center for Analysis and Measurement, Jiaying University, Jiaying, 314001, China

^c College of Materials and Textile Engineering, Jiaying University, Jiaying 314001, China

^d Key Laboratory of the Ministry of Education for Advanced Catalysis Materials, Institute of Advanced Fluorine-Containing Materials, Zhejiang Normal University, 321004, Jinhua, PR China

[#]These authors have contributed equally to this work.

E-mail addresses: liuhaiqing@mail.zjxu.edu.cn (H. Liu), xiaoq@zjnu.edu.cn (Q. Xiao), lei.li@mail.zjxu.edu.cn (L. Li)

1. Experimental

1.1 Materials

1-bromodocosane, Sodium hydroxide, concentrated sulfuric acid (H_2SO_4 , 95-98 wt%), 30 wt% H_2O_2 , *N, N*-dimethylformamide (DMF) and ammonium hydroxide ($\text{NH}_3 \cdot \text{H}_2\text{O}$, 25-28 wt%), Polyvinyl pyrrolidone (PVP, $M_w = 1\,300\,000$) were purchased from Aladdin Chemical Reagent Co. Ltd., China. *N, N, N', N'*-tetramethyl-1, 6-diaminohexane, 1-bromohexane, tetraethyl orthosilicate (TEOS) was obtained from Sigma-Aldrich Co. Ltd. Deionized (DI) water from a Milli-Q system was used, and 1-bromodocosane was bought from TCI chemicals. Celgard 2320 was used as the comparison separator.

1.2 Synthesis of ML-MFI

ML-MFI zeolite was prepared according to the previous report.¹⁻³ Briefly, di-quaternary ammonium-type surfactant [$\text{C}_{22}\text{H}_{45}\text{N}^+(\text{CH}_3)_2\text{-C}_6\text{H}_{12}\text{-N}^+(\text{CH}_3)_2\text{-C}_6\text{H}_{13}$](Br_2) ($\text{C}_{22-6-6}\text{Br}_2$) synthesized by alkylation of *N, N, N', N'*-tetramethyl-1,6-diaminohexane with 1-bromodocosane and 1-bromohexane was used as organic structure directing agent (OSDA). TEOS was hydrolyzed in the presence of OSDA, NaOH, Na_2SO_4 and DI water, followed by crystallization in a rotating Teflon-lined steel autoclave at 150 °C for 7 days. After that, the product was centrifugated, washed with DI water and dried to obtain the ML-MFI zeolite.

1.3 Preparation of open-pore 2D MFI nanosheets (NSs)

Fresh piranha solution (mixture of $\text{H}_2\text{SO}_4/\text{H}_2\text{O}_2$, 3/1, v/v) was used to decompose the OSDA in ML-MFI at 80 °C for 24 h for 4 times. Typically, after dispersing ML-MFI zeolite in H_2SO_4 in a high-temperature bottle with ultrasonication for 30 min,

H₂O₂ was added dropwise to the bottle in a fume hood. The suspension was mixed and stirred for 3 h accompanying by venting occasionally. After tightening the cap, the bottle was placed into an 80 °C oven for oxidation and digestion for 24 h. Then, the suspension was carefully transferred to a centrifuge tube and washed with DI water after completely cooling down to room temperature. The supernatant was discarded and the bottom wet mud was left. Finally, the resultant wet mud was repeatedly treated with piranha solution for 3 times according to the previous steps. After OSDA removal, the wet mud dispersing in DI water was exfoliated by the ultrasonic treatment at 45 kHz for 10 h and subsided for 7 days, yielding the open-pore 2D MFI NSs.

1.4 Preparation of MFI NSs/PAN fibrous membrane

PAN was added evenly into DMF and mechanical stirred for 12 h, obtaining 8 wt% PAN solution. Electrospinning process of PAN solution was performed as follows: feed rate of 2.0 mL h⁻¹, high voltage of 25 kV, collection distance of 20 cm, temperature at 23 ± 1 °C and humidity of 45 ± 3%. The resultant PAN fibrous membrane was dried at 80 °C under vacuum for 12 h before further use. Open-pore 2D MFI zeolite NSs (2 mg) was dispersed in water and 0.2 mg PVP was added, using as filtration suspension. After that, filtration suspension was vacuum filtrated on the surface of as-prepared PAN fibrous membrane using a homemade suction filter with pressure below 0.0005 MPa, obtaining the open-pore MFI NSs/PAN fibrous membrane after drying at 70 °C under vacuum for 12 h. For comparison, MFI nanoflowers (NFs) were prepared via exfoliating as-prepared ML-MFI by the

ultrasonic treatment at 45 kHz for 10 h and subsided for 7 days. MFI NFs/PAN fibrous membrane was prepared by vacuum filtrating MFI NFs suspension composed of MFI NFs (2 mg) and PVP (0.2 mg) on the surface of PAN fibrous membrane. And MFI NSs/Celgard membrane was prepared by vacuum filtrating MFI NSs suspension composed of MFI NSs (2 mg) and PVP (0.2 mg) on the surface of Celgard membrane.

1.5 Characterization

Morphology was observed by a scanning electron microscope (SEM, S-4800) operating at 10 kV. XRD patterns were performed on a Bruker D8 diffractometer with a Cu K α radiation at 3.6° min⁻¹. Transmission electron microscopy (TEM) image was performed on a JEM-2100 equipped with a field emission gun at 200 kV. Pore size distribution was investigated by a CFP-1100AI capillary flow porometer. Porosity and electrolyte uptake were respectively measured using the oil adsorption and the liquid electrolyte adsorption methods as previously reported.^{4, 5} An XQ-1C tensile tester was used to measure the tensile property.⁶ Thermal stability measurements were tested by a differential scanning calorimetry (DSC) and a thermogravimetric analyzer (TGA) in N₂ atmosphere from 50 °C respectively to 350 °C and 750 °C. Thermal shrinkage was evaluated by storing the related membrane at 200 °C for 30 min.

1.6 Electrochemical performance evaluation

Ionic conductivity (σ) was measured on a stainless steel (SS)/separator/SS cell with a frequency range of 0.1-10⁶ Hz and calculated as reported in our previous works. Electrochemical stability window was tested on a SS/separator/Li cell from 2.5 to 6.0 V.⁷ Long-term galvanostatic test of symmetric cells was performed at 2 mA cm⁻² with

capacity of 2 mAh cm^{-2} . For testing the cell performance, the CR 2016 cell was assembled in a glovebox filled with argon by placing the separator between LiFePO_4 cathode (LiFePO_4 /carbon black/PVdF, 7/2/1, weight ratio) with a mass loading of $0.98\text{-}1.04 \text{ mg cm}^{-2}$ and lithium metal anode. The cell performances were carried out with Land CT 2001A battery tester. The galvanostatic cycling performance of the Li/Li symmetric cells assembled with different separators were carried out at current density of 2 mA cm^{-2} . Coulombic efficiency of the Cu/Li asymmetrical cells assembled with different separators were tested at 1 mA cm^{-2} with a capacity of 1 mAh cm^{-2} . The electrolyte used for Li/ LiFePO_4 and Li/Li cells were $1 \text{ mol L}^{-1} \text{ LiPF}_6$ in ethylene carbonate/dimethyl carbonate/ethyl methyl carbonate (1/1/1, w/w/w), while the electrolyte used for Cu/Li cells were 1.0 M LiTFSI in a mixture of 1,3-dioxalane and dimethylether (1:1, V/V) with 2 wt% LiNO_3 additive.

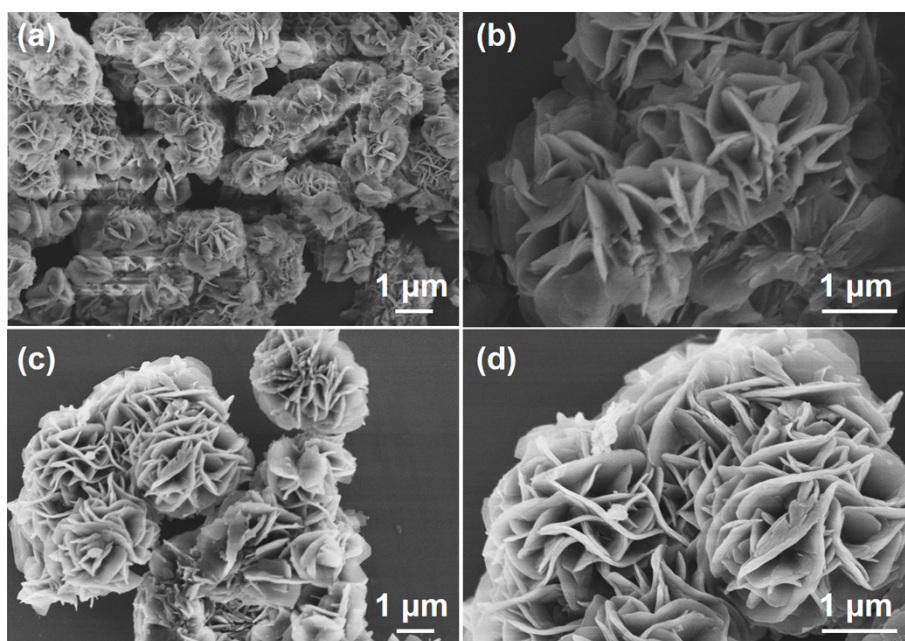


Fig. S1 SEM images of (a, b) ML-MFI and (c, d) MFI nanoflowers.

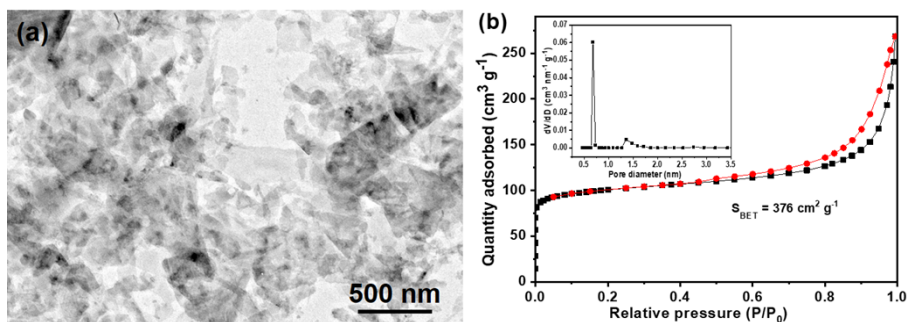


Fig. S2 (a) TEM images and (b) N_2 adsorption-desorption isotherm of open-pore MFI NSs.

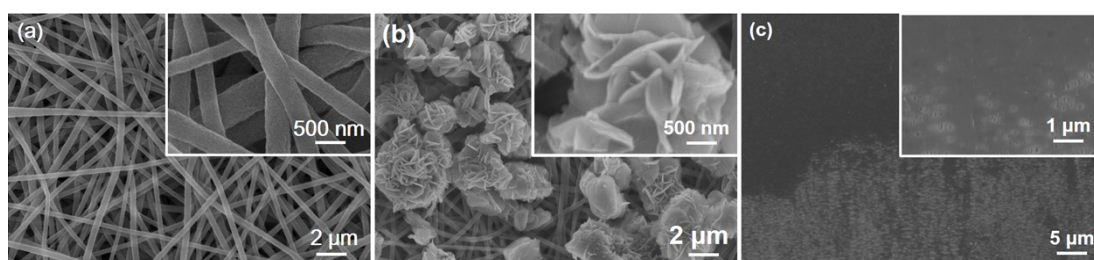


Fig. S3 SEM images of (a) PAN, (b) MFI NFs@PAN and (c) MFI NSs@Celgard separators.

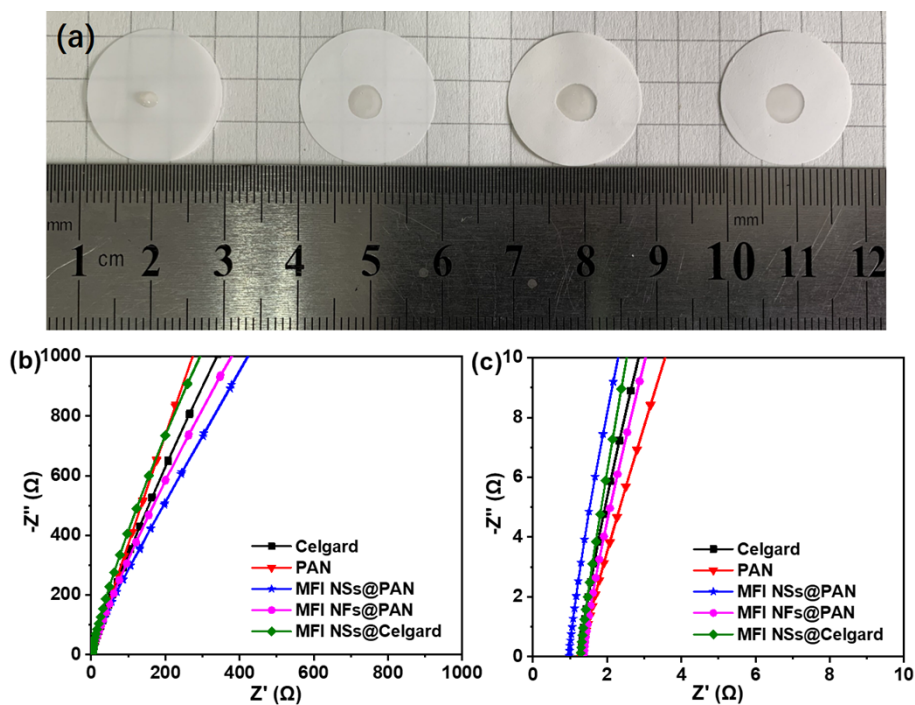


Fig. S4 Photos of relevant separators (a) wetted by $1 \mu\text{L}$ electrolyte, and (b, c) Nyquist plots of relevant separators.

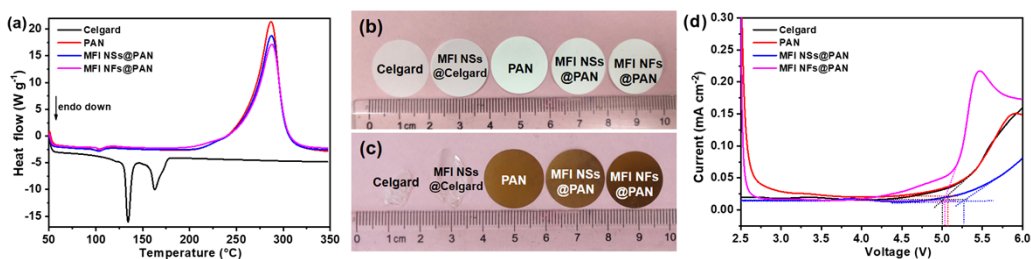


Fig. S5 (a) DSC curves of relevant separators, Photos of relevant separators (b) before and (c) after heating at 200 °C for 0.5, (d) LSV curves of relevant separators.

In LSV curves, the voltage at which the current begins to increase steadily indicates the oxidative decomposition potential of the relevant separator. In general, the electrochemical oxidation limit is determined by the oxidative decomposition of the free solvent molecules in electrolyte and the destruction of electrode materials.⁸ Elevating the electrolyte storage ability of separator and then reducing the direct contact of electrolyte and cathode is an effective way to alleviate the decomposition of free solvent molecules.⁹ The improved oxidation stability of MFI NSs@PAN separator is primarily attributed to the largely increased uptake. The nanofluid channels in the MFI NSs coating layer provide more liquid storage pools that reduce the leakage of electrolyte, eventually alleviating the contact of free solvent molecules with cathode. Moreover, the removing trace impurities ability of MFI NSs could also enhance the anodic stability of MFI NSs@PAN separator.

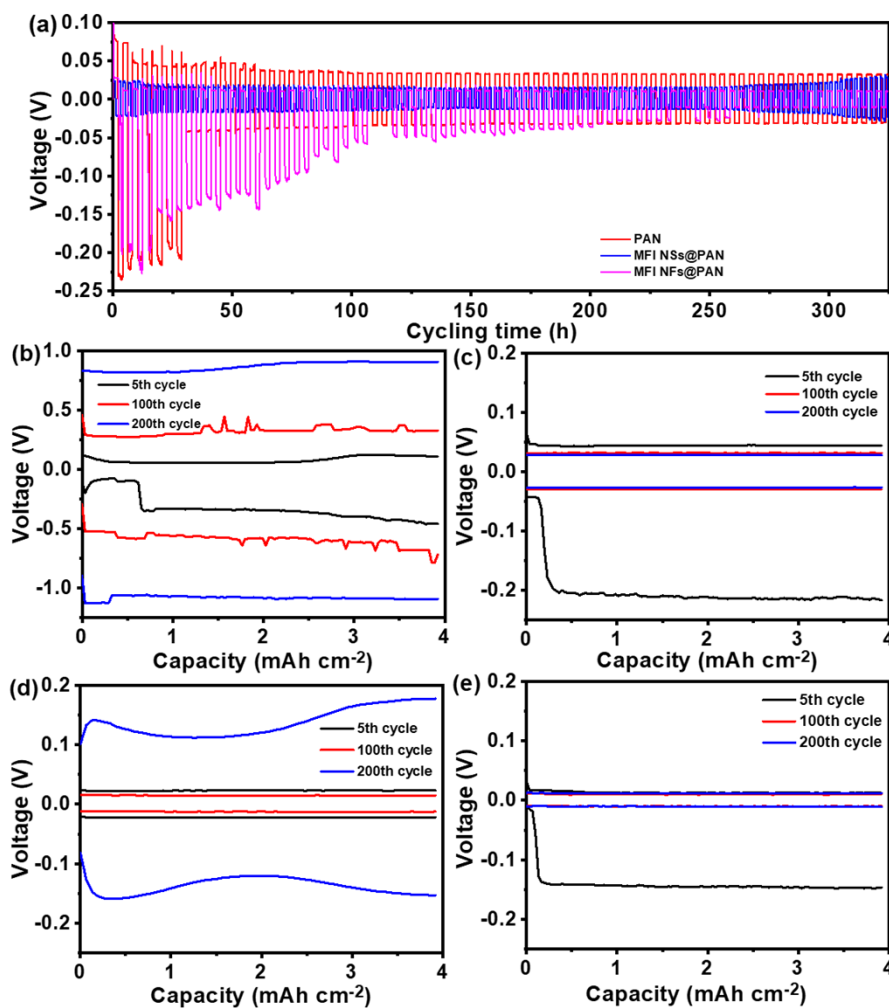


Fig. S6 (a) Voltage-time profiles of Li plating/stripping processes in the y-axis range between 0.1 and -0.25 V. Voltage profiles of the Li/Li cells with (a) Celgard, (b) PAN, (c) MFI NSs@PAN and (d) MFI NFs@PAN separators.

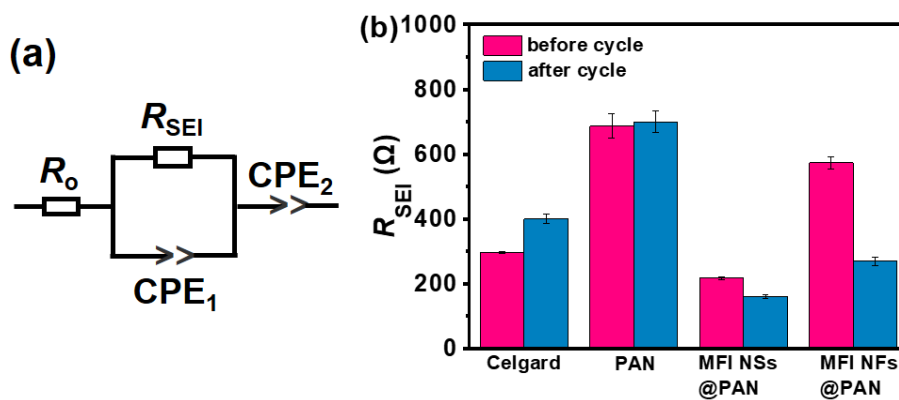


Fig. S7 (a) EIS equivalent circuit and (b) Comparison of R_{SEI} fitting results of the cells using relevant membranes before and after 300 cycles.

In the equivalent circuit, R_o represents the cell resistance, R_{SEI} denotes the resistance for Li^+ migration through higher SEI film, CPE_1 and CPE_2 correspond to the space-charge capacitance of SEI films at Li/electrolyte interface and the double-layer capacitance at the $LiFePO_4$ /electrolyte interface, respectively.

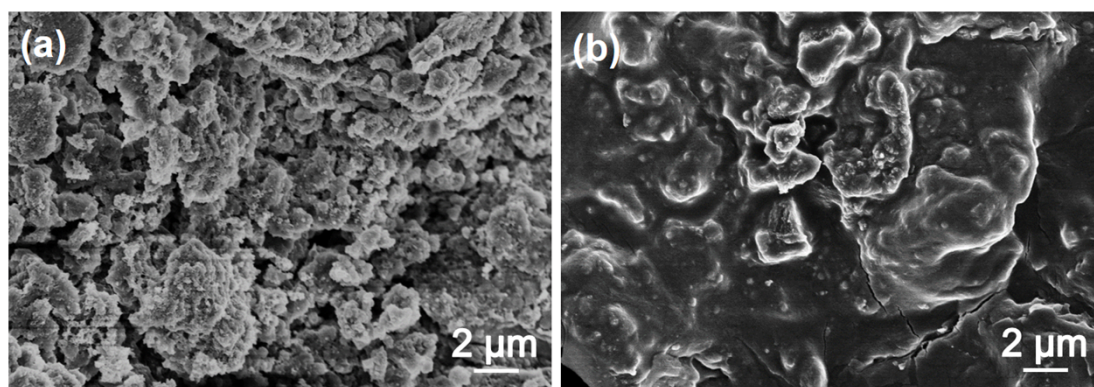


Fig. S8 SEM images of Li anodes in Li/LiFePO₄ cell with (a) Celgard and (b) MFI NFs@PAN separators after 300 cycles.

Table S1 Physical parameters of the relevant separators.

Samples	Porosity (%)	Electrolyte uptake (%)	Bulk resistance (Ω)	Ionic conductivity ($mS\ cm^{-1}$)
Celgard	44.1	129	1.30	0.74
MFI NSs@Celgard	40.6	116	1.27	0.80
PAN	82.1	288	1.31	1.30
MFI NSs@PAN	71.9	264	0.97	1.90
MFI NFs@PAN	63.2	200	1.43	1.29

Table S2 Electrochemical performance comparisons between MFI NSs@PAN and other nanoporous separator/interface for stable Li anode.

Separator/interface	Li/Li	Cu/Li (1 mA/cm ² -1 mAh/cm ²)	LFP/Li
PMOF80 ¹⁰	100 mV for 650 hours at 0.5 mA/cm ² -1 mAh/cm ²	-	5C: about 90 mAh/g 1C: 135 mAh/g 85% retention after 400 cycles at 1C 0.2C: 163 mAh/g
SAMsC ¹¹	40 mV for 2500 hours at 1 mA/cm ² -1 mAh/cm ²	CEs of 97.7% over 300 cycles	3C: 137 mAh/g 80% retention after 450 cycles at 1C
UiO-66 ¹²	100 mV for 530 hours at 1 mA/cm ² -1 mAh/cm ²	-	- 0.05C: 152 mAh/g
MCM/PVDF/PPnw ¹³	150 mV for 225 hours at 0.4 mA/cm ² -0.4 mAh/cm ²	-	0.5C: 10 mAh/g 96.9% retention after 100 cycles at 0.1C
COF-F@PP ¹⁴	18 mV for 1100 hours at 1 mA/cm ² -1 mAh/cm ²	CEs of 95% over 90 cycles with retention of 96.6%	1C: 141 mAh/g 10C: 84.5 mAh/g 95.3% retention after 450 cycles at 1C
MFI NSs@PAN	20 mV for 325 hours at 2mA/cm ² -2 mAh/cm ²	CEs of 98% over 100 cycles with retention of 96.6%	0.1C: 148 mAh/g 14C: 94 mAh/g 2C: 94% retention after 300 cycles at 2C

References

- 1 H. Zhang, Q. Xiao, X. Guo, N. Li, P. Kumar, N. Rangnekar, M. Y. Jeon, S. Al-Thabaiti, K. Narasimharao, S. N. Basahel, B. Topuz, F. J. Onorato, C. W. Macosko, K. A. Mkhoyan and M. Tsapatsis, *Angew. Chem. Int. Ed.*, 2016, **55**, 7184-7187.
- 2 M. Choi, K. Na, J. Kim, Y. Sakamoto, O. Terasaki and R. Ryoo, *Nature*, 2009, **461**, 246-249.
- 3 K. Varoon, X. Zhang, B. Elyassi, D. D. Brewer, M. Gettel, S. Kumar, J. A. Lee, S. Maheshwari, A. Mittal, C.-Y. Sung, M. Cococcioni, L. F. Francis, A. V. McCormick, K. A. Mkhoyan and M. Tsapatsis, *Science*, 2011, **334**, 72.
- 4 D. Lin, D. Zhuo, Y. Liu and Y. Cui, *J. Am. Chem. Soc.*, 2016, **138**, 11044-11050.
- 5 K. Xiao, Y. Zhai, J. Yu and B. Ding, *RSC Adv.*, 2015, **5**, 55478-55485.
- 6 Y. Zhai, N. Wang, X. Mao, Y. Si, J. Yu, S. S. Al-Deyab, M. El-Newehy and B. Ding, *J. Mater. Chem. A*, 2014, **2**, 14511-14518.
- 7 H. Liu, X. Wang, C. Kuang, L. Li and Y. Zhai, *J. Solid State Electrochem.*, 2018, **22**, 3579-3587.
- 8 T. Ma, Z. Cui, Y. Wu, S. Qin, H. Wang, F. Yan, N. Han and J. Li, *J. Membr. Sci.*, 2013, **444**, 213-222.
- 9 Y. Li and H. Pu, *J. Power Sources*, 2018, **384**, 408-416.
- 10 Z. Li, Q. Liu, L. Gao, Y. Xu, X. Kong, Y. Luo, H. Peng, Y. Ren and H. Wu, *J. Energy Chem.*, 2021, **52**, 354-360.
- 11 Y. Liu, X. Tao, Y. Wang, C. Jiang, C. Ma, O. Sheng, G. Lu and X. Lou, *Science*, 2022, **375**, 739-745.
- 12 Y. Xu, L. Gao, L. Shen, Q. Liu, Y. Zhu, Q. Liu, L. Li, X. Kong, Y. Lu, and H. Wu, *Matter*, 2020, **3**, 1685-1700.
- 13 Z. Chen, Y. Xu, W. Zhao, Q. Liu, Q. Liu, Z. Hu, Y. Liu and H. Wu, *Chem. Commun.*, 2022, **58**, 13656-13659.
- 14 S. Yao, Y. Yang, Z. Liang, J. Chen, J. Ding, F. Li, J. Liu, L. Xi, M. Zhu and J. Liu, *Adv. Funct. Mater.*, 2023, **33**, 2212466.